Available online at www.sciencedirect.com
SCIENCE DIRECT®
PERGAMON
Engineering Failure Analysis □ (□□□□) □–□
ENGINEERING FAILURE ANALYSIS
www.elsevier.com/locate/engfailanal

Failure of locked coil wire rope of coal handling system

P. Parameswaran[a,*], V.S. Raghunathan[a], S.C. Hiremath[b], K.R. Paknikar[c]

[a]Materials Characterisation Group, Indira Gandhi Centre for Atomic Research, Kalpakkam 603 102, India
[b]Heavy Water Board, Mumbai 400 094, India
[c]Heavy Water Plant, Manuguru, Andhra Pradesh 507 116, India

Received 22 October 2002; accepted 18 January 2003

Abstract

The outer Z-shaped wires of locked coil wire ropes used in coal transportation were found to fail frequently. A systematic metallographic investigation was carried out to understand the cause of failure. The wire was found to fail due to decarburised layers that form due to improper heat treatment procedure followed during production. The steps to avoid decarburisation and a comprehensive mechanical test were suggested to ascertain the life of the wire ropes.

Keywords: Rope failures; Decarburisation; Heat treatment; Annealing; Fatigue

1. Introduction

An aerial steel wire rope system is employed in transporting about 300 MT of coal per day. The wire rope system consists of 64 mm diameter locked coil steel wire ropes. These ropes support the ~125 buckets each of 1500 kg of coal at a time. The wire ropes are supposed to serve the intended service life of 5–7 years. Fig. 1 shows the schematic arrangement of the wire rope construction, which consists of central round wires of different radii and outer Z wires. However, failure occurred quite often over a span of few weeks on the outer Z wire of the wire rope. An investigation of wire rope samples, from ropes that served a complete period of 7 years, corresponding unused wires and a similar set of samples from wires that failed frequently was carried out to obtain an understanding on a comparative basis.

2. Experimental

The samples of wire ropes that completed their intended life span are referred as WS1 and unused wire samples as WS2. The samples corresponding to ropes with poor-service life are referred as PS1 and the corresponding unused wire samples as PS2.

* Corresponding author. Tel.: +91-4114-280-306; fax: +91-4114-280-080.
E-mail address: param@igcar.ernet.in (P. Parameswaran).

1350-6307/03/$ - see front matter © 2003 Elsevier Science Ltd. All rights reserved.
doi:10.1016/S1350-6307(03)00019-0

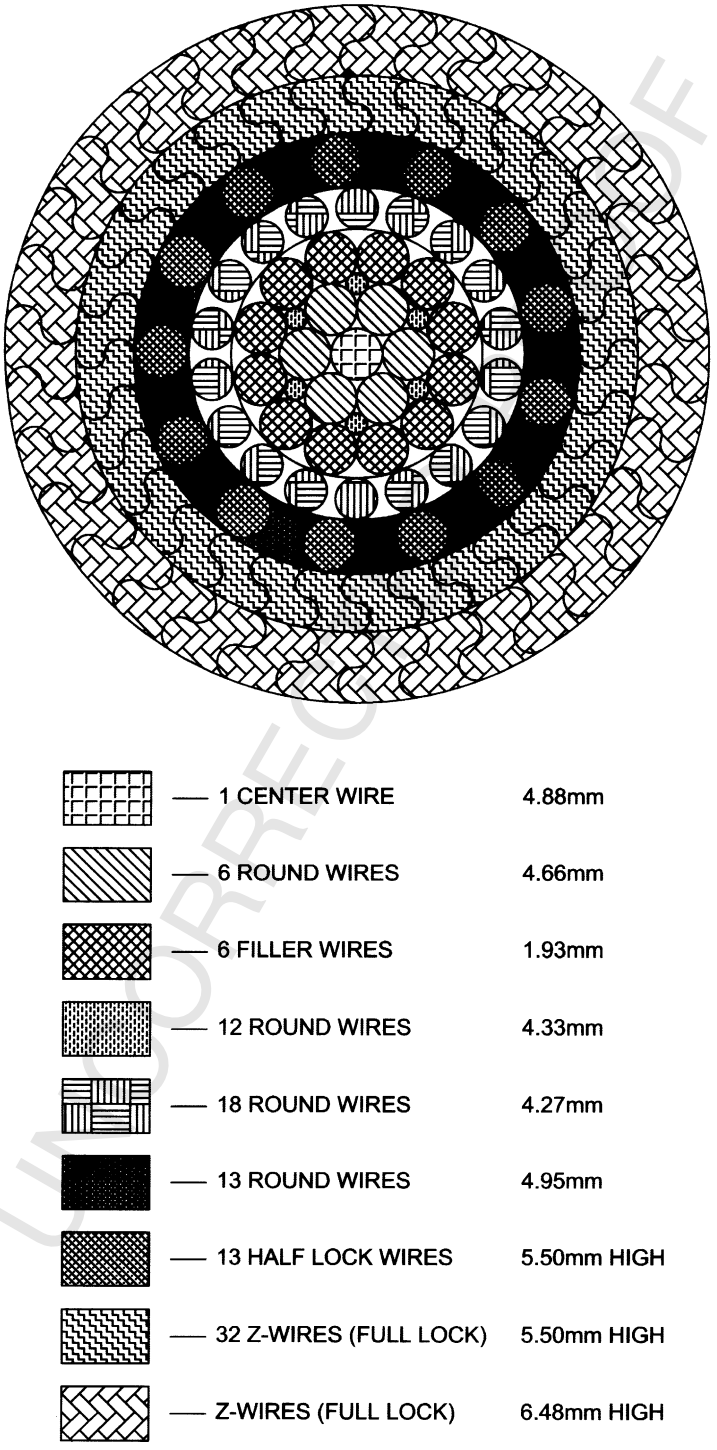

Fig. 1. Schematic figure depicting the wire construction.

The composition of the steel wire is shown in Table 1. Transverse as well as longitudinal cross sections from the wires are cut; the transverse sample has been identified into three regions of different cross section, namely—the large flange (LF), rib and small flange (SF) (see Fig. 2). The samples were polished and etched with 1%Nital and examined for metallographic observation in an optical microscope, model MeF4A (M/s. Leica, Austria).

Macrohardness values were taken using 10 kg load to get the overall hardness of all the three samples. The microhardness of subsurface and different sections like rib and flange representing the interior was taken with 50 g load. A 25 g load was used to examine the surface layers. Fractured surfaces were examined using scanning electron microscopy (SEM). In addition, the cross-sections of the fracture surfaces were examined by optical microscopy.

3. Results

3.1. Microstructural and microhardness studies

Optical microscopic investigation of the transverse and longitudinal sections of the samples indicates that the general microstructure is drawn pearlitic in nature (Fig. 3). However, careful examination of the sample of the wire that served a shorter life (PS2) indicated that the microstructure along the surface changes to ferrite, indicating the possibility of a decarburised layer. Hence the microhardness of the cross section of the samples was measured. Fig. 4 presents the hardness values as a profile for all the different sections of WS2 and PS2 samples. The microhardness of WS2 remained almost constant around the surface layers in all three sections. In contrast, the surface layers of the rib section of sample PS2 exhibited a hardness of 250 VHN. This is in contrast to the core hardness, which is around 330–350 VHN. On examining several locations near the surface of the rib section, the hardness was found to be around 190–250 VHN. This confirms that a decarburised layer of 40 μm exists around the surface of PS2.

Table 1
Composition of the steel used for the manufacture of the wire rope

Elements	C	Mn	Si	S	P
Wt.%	0.70	0.77	0.17	0.003	0.015

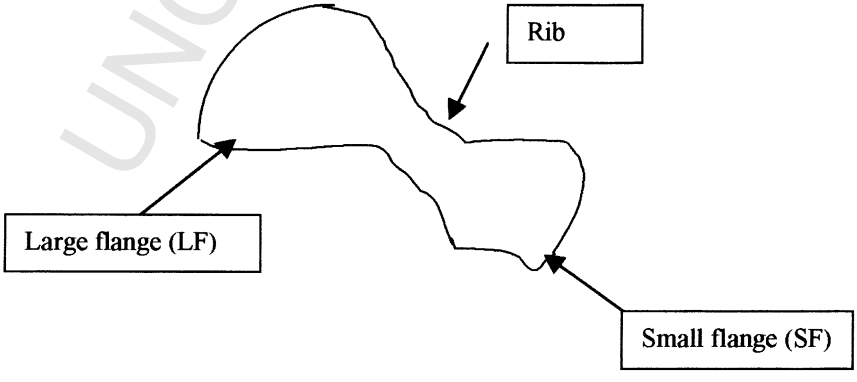

Fig. 2. Schematic sketch of the cross section of the outer Z-wire.

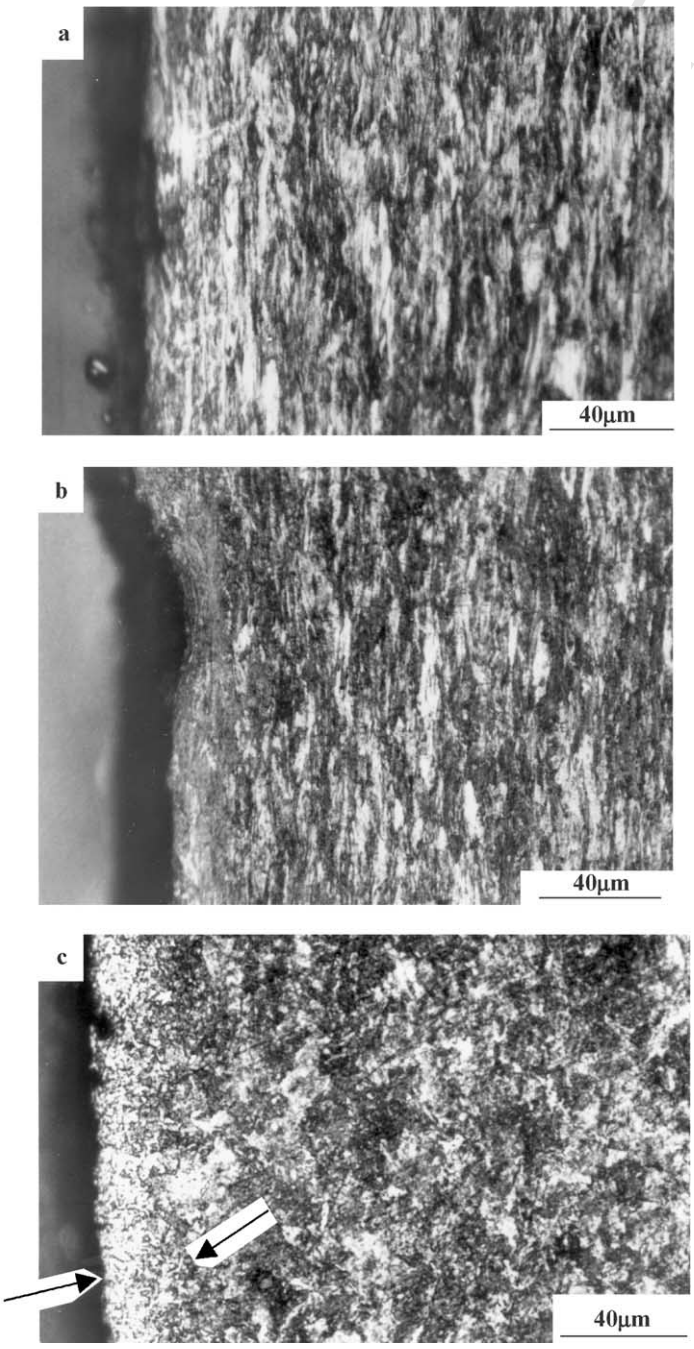

Fig. 3. Optical micrographs of the transverse section of samples (a) WS1, (b) WS2, (c) PS2. In all the samples, generally the structure is drawn pearlitic in nature. Arrows in (c) refer to the decarburised layer.

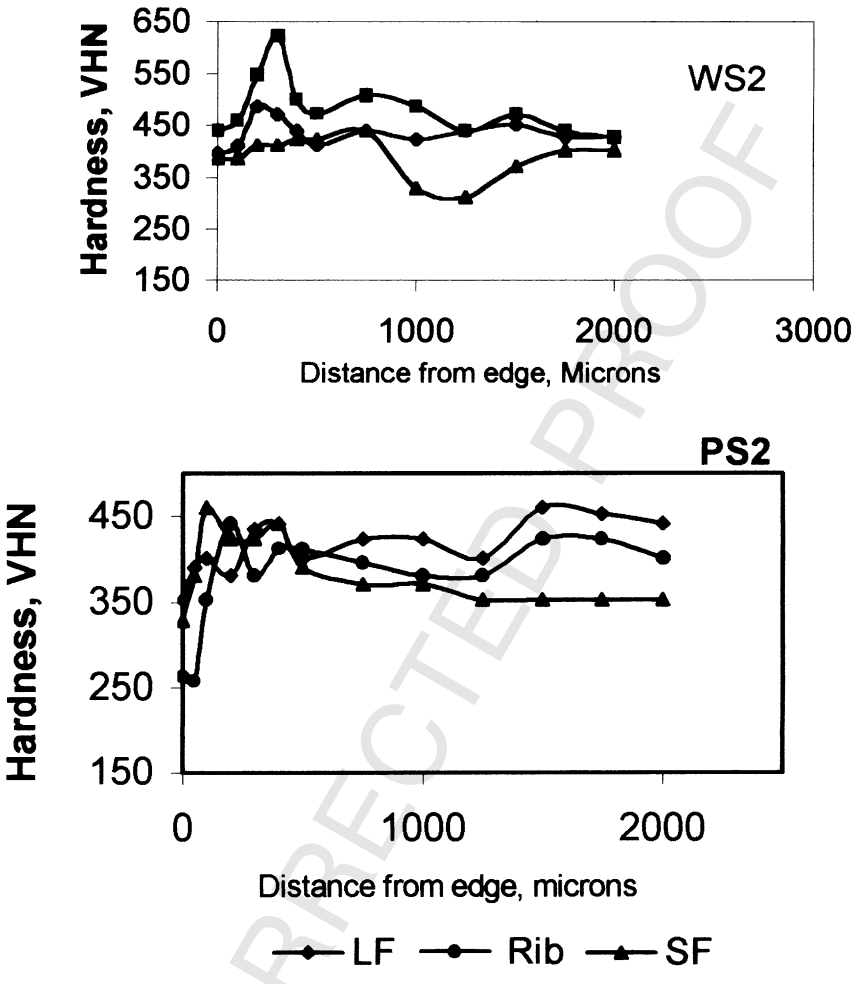

Fig. 4. Microhardness profile of the samples WS2 and PS2 samples for different regions of the cross sections of the wire. Note the sample PS2 shows a low surface hardness in the rib region.

3.2. Fractographic studies

The fractured surfaces of the two samples, PSI and WSI, were studied using SEM.

The failed surface of sample PS1 exhibited a crack origin (A) on the edge in the rib location of the cross section (Fig. 5). A higher magnification view (a) of the area A shows clearly round crack fronts (arrow) with fine voids. The crack origin shows shear lips emanating out from the surface edges. This means there is a region of severe plastic yielding around this area. Our earlier finding that a decarburised zone exists around the edges is in line with the present observation. This is a typical case of fatigue failure, developed at the soft surface layers and propagated slowly.

The circular crack front, which emerged from the location A is observed to go into the small flange area in the form of circular lines with cavities. Further secondary cracks (B) generated therein and overload fracture appeared (C). Consequently, on the other end, which is at the large flange, a crack opened up with very flat fractured area (E). In order to confirm the role of the decarburised layer, cross-sectional micro-

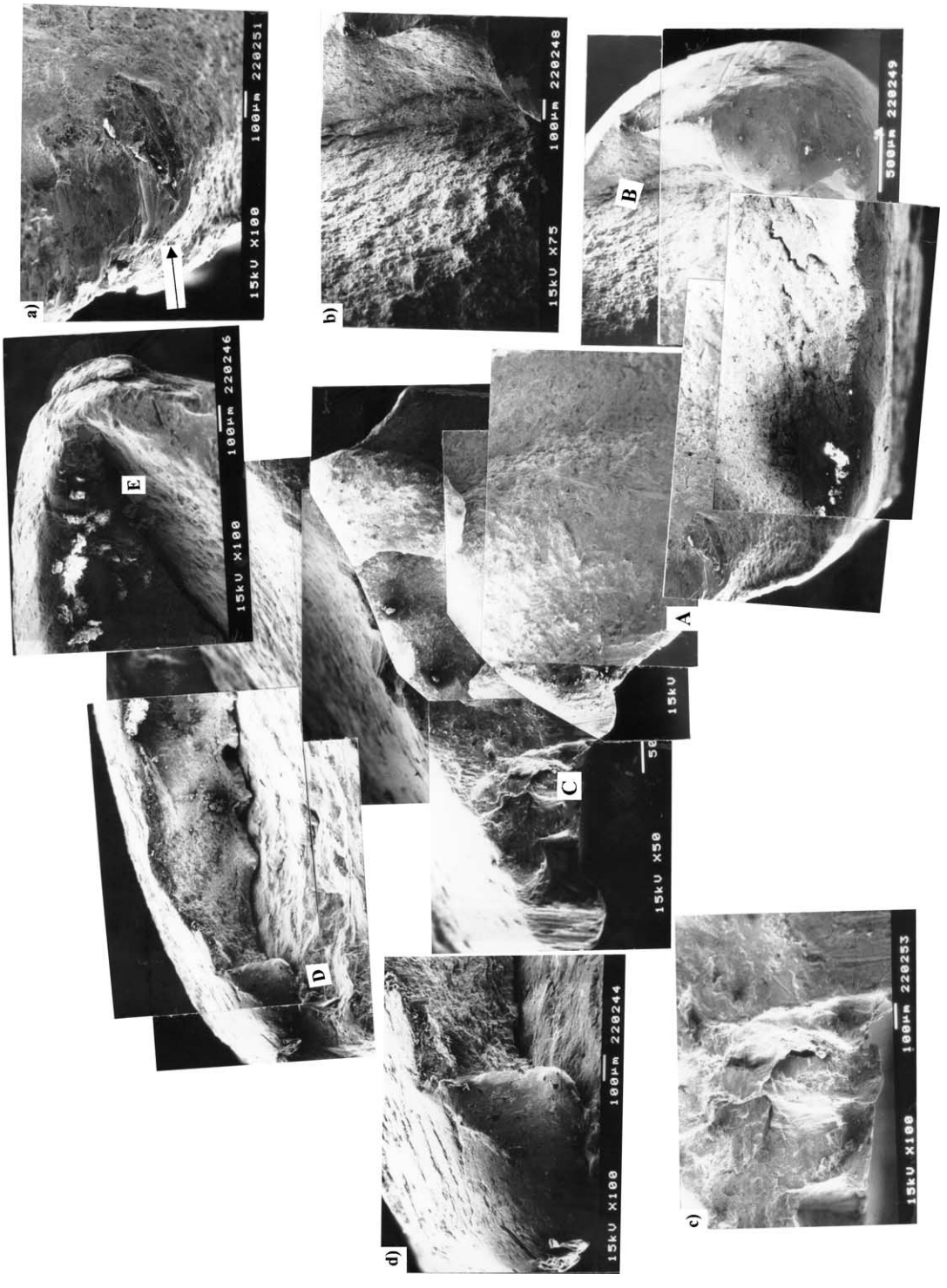

Fig. 5. SEM fractograph as a montage showing details of fracture of sample PS1. Regions A, B, C, D in the montage are shown in a detailed view in (a), (b), (c) and (d). Region A is origin. B refers to secondary cracks4E refers to overload failure. Arrowhead shows the crack front developing as circular lines from the origin A.

scopy of the same sample was carried out. Fig. 6 shows the optical microscopy of the rib region of the wire. It can be easily observed from the figure that the crack has originated in the decarburised zone.

Fig. 7 shows the fractographic details of sample WS1. The origin of the crack begins at the edge of the large flange (see arrow). Then a crack front develops with steps (S1, S2). There are also ductile fibres (D) which seem to go into the rib. However, the rib contains oriented grains leading to secondary cracking [see fine parallel lines (E)]. The load bearing area being less, overload fracture occurred (located at the centre with a deep cavity evident there).

Thus, the fracture surface details clearly indicate fatigue-loading signatures like concentric lines developing from the origin in the case of sample PS1, along with ductile dimples. This could happen in case of constant tension loading superimposed with an impact load.

The fracture surface of wire sample WS1 indicated the failure originated from the surface with its development continuing with steps. These are again signatures of fatigue. However, the wire seems to have been subjected to large ductile deformation, as indicated by ductile fibres in the rib section. This is due to the strengthening effect of the oriented grains.

4. Discussion

During service, the wire was subjected to a constant tensile load due to clamping. In addition the rope experiences an impact load at a frequency of the passage of buckets. Based on the data of the bucket movement, this is approximately 20 s between the passage of successive buckets. This would mean that a fatigue loading would be seen a million times a year. This sort of fatigue loading could initiate cracks in the decarburised layers, which act as metallurgical stress raisers [1], since decarburised zones are considered similar to rough surfaces. The response of mixed microstructure to fatigue loading has been studied [2], and it is expected that decarburised zone at the surfaces is likely to see a higher amount of strain compared to interior regions.

During the manufacturing stages of the ropes, annealing is the most probable source of decarburisation. It is the annealing treatment step for which a four-zone retort furnace is employed. Propane gas is used to heat the wires. The wire move through the furnace at a pre-determined speed to ensure the annealing or heat treatment time is as desired. A few important aspects are to be considered during annealing.

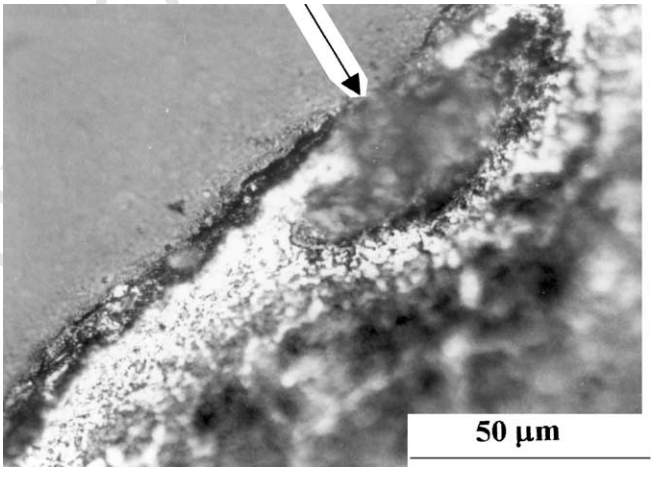

Fig. 6. Optical micrograph of the cross section of the failed wire showing the Rib section. Note the crack at the decarburised layer.

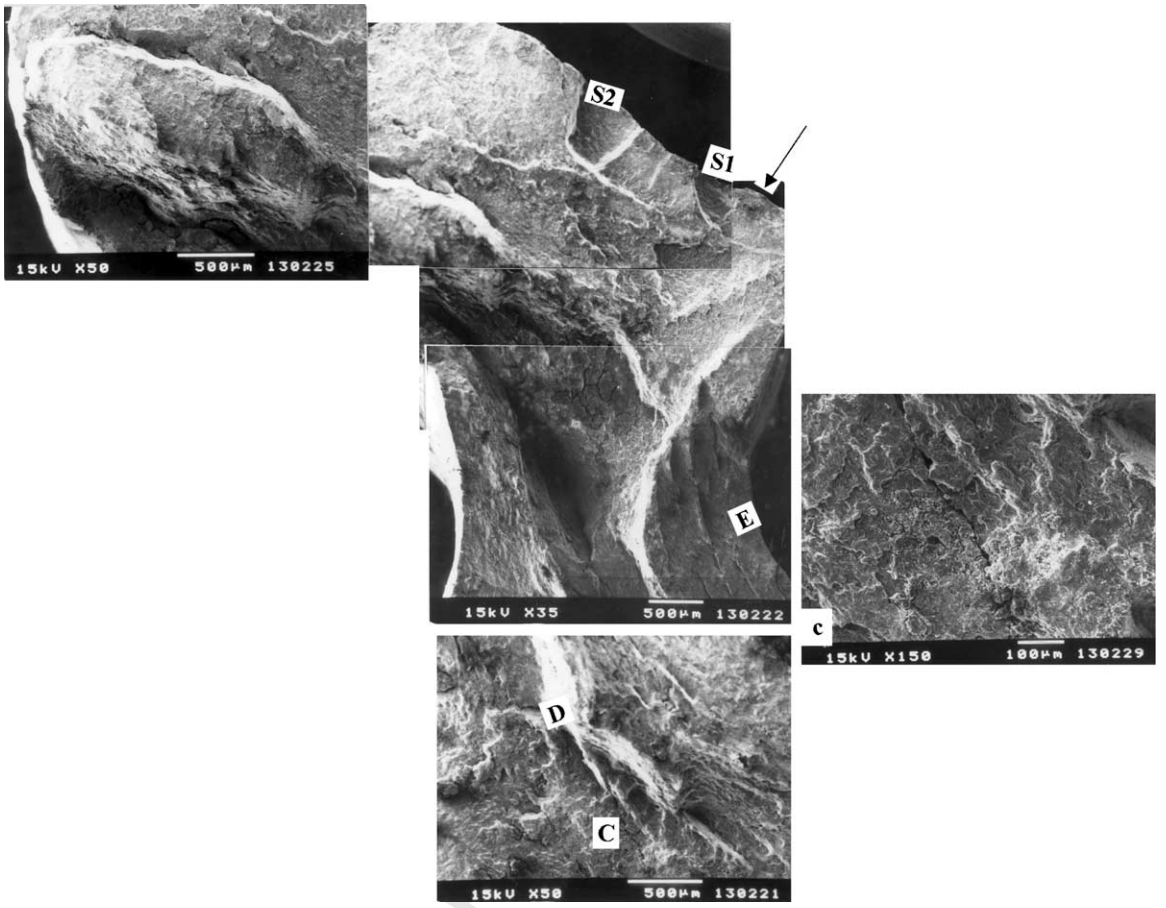

Fig. 7. SEM fractograph as a montage showing%e details of fracture of sample WS1. Note the arrowhead pointing to the origin; see the steps S1, S2, the ductile fibres (D) and the fine lines (E) of the secondary cracks due to oriented grains in the rib region. Region C is shown again in higher magnification.

The furnace atmosphere in these furnaces is a combination of CO_2 and CO. The consequence of this atmosphere is governed by the curves shown in Fig. 8. Two reactions are important in this figure namely, the oxidation of iron by CO_2 occurring for gas compositions and temperatures above and to the left of the curve labelled with the composition in question. For 0.8%C, the furnace atmosphere has to be high in CO content, say of the order of 98% or so, for an annealing temperature of 1020 °C.

If the atmosphere has less than the prescribed proportion of CO, then it will be decarburising [3]. Hence it becomes necessary to control the relative amounts of the two gases to avoid decarburisation. Alternatively, for a given furnace atmosphere, the annealing temperature can be lowered to avoid decarburising.

The time of heat treatment determines the decarburisation reaction and the depth of decarburisation. Assuming the diffusion constant, D to be 10^{-8} cm^2/s [3], the depth of decarburised layer, d_c can be calculated through the formula:

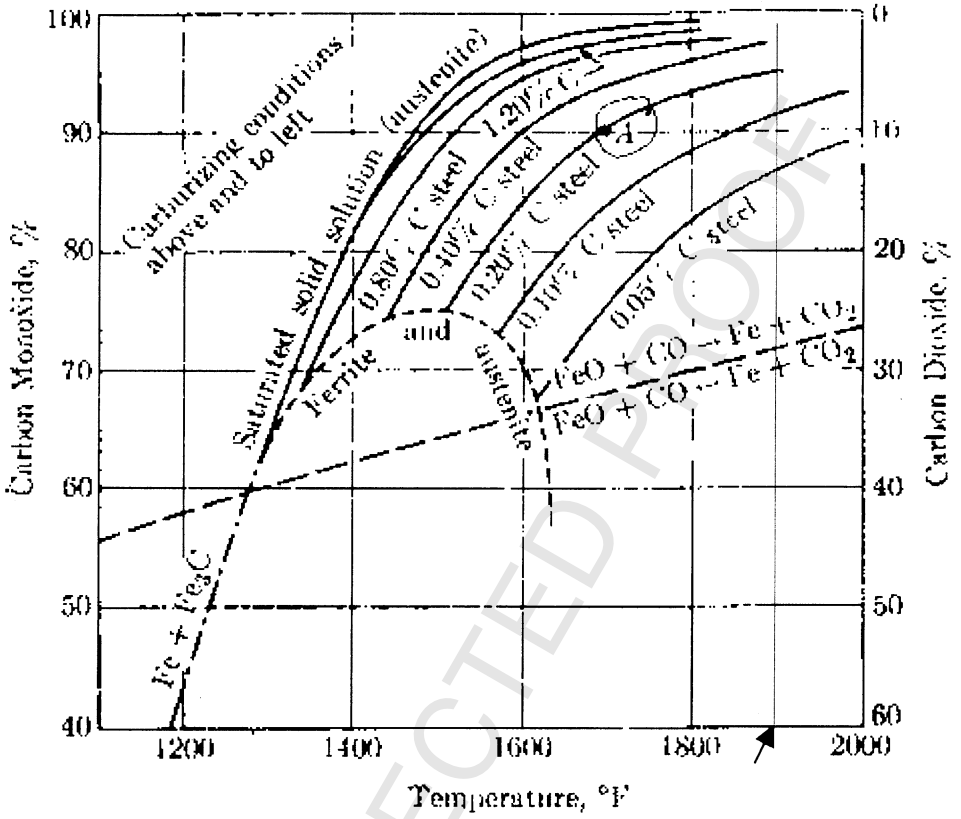

Fig. 8. Curves showing the equilibrium between CO-CO_2 gas mixtures and steels of various carbon contents at heat treating temperatures [3]. Note the arrow indicates the temperature of annealing. It can be read that the corresponding amount of CO should be around 98%.

$$d_c = 2\sqrt{Dt} \tag{1}$$

then for 1 min

$$d_c = 2\sqrt{(10^{-8} \times 60)} \sim 16 \times 10^{-4}\text{cm} = 16\ \mu\text{m}. \tag{2}$$

This compares well with the observed value of ~40 μm, if we assume a heat treatment time of a few minutes. Hence the heat treatment at high temperatures in the given furnace atmosphere could lead to considerable decarburisation. To overcome this effect, it is necessary to reexamine this heat treatment schedule.

4.1. A quality assurance step

In addition to microstructural quality assurance, it is felt that a comprehensive mechanical testing procedure is essential. Regular mechanical testing of individual wires is employed to ascertain fatigue and tensile properties. These results generally indicate better properties for the wires. However, considering the fact that wires after rope manufacture would behave in an integrated fashion, the testing of the full size rope with a loading cycle simulating the service load condition is useful. Accordingly, it is suggested that a

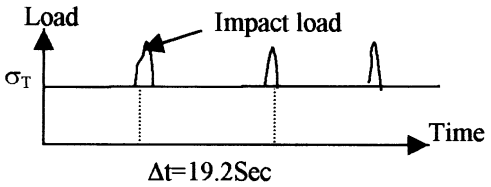

Fig. 9. Schematic of a mechanical test involving a constant tensile load with an impact load at a frequency of bucket movement.

test to impose a constant tensile load with an impact load on a standard pre-determined length of the rope could be most beneficial. Fig. 9 depicts the schematic of such a test The frequency of the impact load is approximately the 0.02 Hz ($\sim 10^6$/year). This test is recommended to be added in the specification.

5. Conclusions

1. Microscopic, microhardness and fractography investigations on failed wires of locked coil wire ropes were carried out.
2. Microscopic and microhardness studies indicate that decarburisation occurs during annealing treatment of the wires. This leads to a soft surface layer, which is a potential fatigue crack initiation site.
3. Fractography confirms cracks emanating from the surface layers exhibiting extensive deformed layers. This indicates the role of decarburised layers in starting fatigue cracks.
4. To avoid decarburisation, it is necessary to have a close control of the furnace atmosphere by checking the relative partial pressures of CO_2 and CO. Alternatively given a furnace atmosphere, decarburisation can be avoided by lowering the annealing temperature.
5. A comprehensive mechanical testing of the fully locked wire rope subjected to tension–impact loading is suggested to ascertain the expected life of the rope.

References

[1] Dieter, G.E. Mechanical metallurgy. McGrawHill, Inter. Student ed; 1976.
[2] Pedersen K, Helgeland O, Lohne O. In: Proc. of the 4th European Conf on Fatigue and Fracture, held in Leoben, Austria. 1982, p. 495.
[3] Guy AG. Physical metallurgy. Calcutta, India: Oxford and Indian Book House Publishing Co; 1967.